Access Delay of Cognitive Radio Networks Based on Asynchronous Channel-Hopping Rendezvous and CSMA/CA MAC

Quan Liu, *Student Member, ACM,* Xudong Wang, *Senior Member, IEEE,* Biao Han, *Student Member, IEEE,* Xiaodong Wang, *Member, IEEE,* and Xingming Zhou

***Abstract*—As a promising approach to the rendezvous problem in cognitive radio networks (CRNs), blind rendezvous paradigm recently spawns various asynchronous channel-hopping (CH) rendezvous schemes that enable any two neighboring secondary users to meet among multiple channels within a finite time even without any synchronization. However, rendezvous delay derived in existing work is unable to reflect the actual channel access delay performance in multi-user CRNs, as it only relies on hopping patterns of the elaborately designed channel-hopping sequences (CHSs) and ignores the impact of network factors (e.g., channel availability and multi-user contention). In this paper, channel access delay is investigated by jointly considering asynchronous CH rendezvous schemes, channel availability, and MAC protocol in a single-hop multi-user CRN. To coordinate multi-user contention, a CSMA/CA MAC is adopted by tailoring IEEE 802.11 distributed coordination function (DCF) properly to the operation features of existing asynchronous CH rendezvous schemes. The channel access delay is analyzed based on a modified Bianchi model and an Absorbing Markov Chain model, which captures the aggregate effect of hopping patterns of CHSs, the dynamic nature of channel availability, and the behavior of the MAC protocol. The analytical results are verified through extensive simulations. Both simulation and analytical results reveal that the rendezvous delay in existing asynchronous CH rendezvous schemes is insufficient to ensure satisfactory channel access delay in multi-user CRNs.**

***Index Terms*—Cognitive Radio Networks, Asynchronous Channel-Hopping Rendezvous, Rendezvous Delay, 802.11 DCF, Channel Access Delay**

I. Introduction

COGNITIVE radio networks (CRNs) [1], which employ cognitive radio technology to make full use of the under-utilized licensed spectrum bands, have made a significant difference to conventional wireless networks. With aim at improving the utilization efficiency of licensed spectrum, secondary users (SUs) hunt for idle spectrum bands through spectrum sensing and exploit these spectrum opportunities offered unintentionally from primary users (PUs) to communicate with each other. In order to avoid harmful interference with PU communications, SUs have to vacate the used spectrum bands immediately when PUs reclaim them. Thus, the dynamic channel[1] availability makes traffic coordination among SUs exceedingly challenging [2], especially in distributed CRNs.

Like in conventional multi-channel networks [3], MAC design in CRNs also encounters a fundamental issue termed as the "*rendezvous*" problem, which refers to how a sender and its intended receiver (i.e., a rendezvous pair) meet among multiple channels. The most intuitive and well-accepted solution is to specify a dedicated channel, i.e., dedicated common control channel (DCCC), for control negotiation between SUs. Due to its simplicity, most distributed MAC protocols [4] employ DCCC to handle the rendezvous problem in CRNs. However, besides the drawbacks (e.g., control channel congestion and vulnerability to attack) discussed in [3] for conventional wireless networks, the DCCC scheme has two distinctive drawbacks for CRNs: (1) *Existence problem*, i.e., the available channel set of a SU depends on its location relative to PUs so that a global available DCCC with network-wide coverage may not exist; (2) *Availability problem*, i.e., the availability of the specified DCCC is uncertain due to PU activity. For these reasons, the rendezvous problem is still regarded as an open problem [5] in CRNs.

Without relying on any preassigned central controller or DCCC, *blind rendezvous* paradigm [6] is preferred in practice. As the most representative technique to realize blind rendezvous, channel-hopping (CH) based rendezvous schemes are researched intensively in these years [7]. Their basic idea is to arrange network channels into a channel-hopping sequence (CHS) and ensure that any two neighboring SUs meet in the same channel by jumping along the designed CHS in a slot-by-slot manner. The advantage of CH based rendezvous schemes is that they are suited to the feature of dynamic channel availability in CRNs and can obtain multi-channel gain by distributing traffic load over different channels. How to guarantee rendezvous among SUs is the major problem in the design of CH based rendezvous schemes. Synchronous CH rendezvous schemes (e.g., L/M-QCH [8] and ETCH-SYN [9]) can not only guarantee rendezvous but also achieve optimal rendezvous delay and load balance, but they require

Quan Liu, Xiaodong Wang and Xingming Zhou are with Science and Technology on Parallel and Distributed Processing Laboratory, School of Computer Science, National University of Defense Technology, Changsha, Hunan, 410073 P.R.China (e-mail: {liuquan, xdwang, xmzhou}@nudt.edu.cn).

Xudong Wang is the corresponding author. He is with the University of Michigan-Shanghai Jiao Tong University Joint Institute, Shanghai Jiao Tong University, Shanghai, 200240 P.R.China (e-mail: wxudong@ieee.org).

Biao Han is with the Graduate School of Systems and Information Engineering, University of Tsukuba, Tsukuba Science City, 305-8573, Japan(e-mail: hanbiao@osdp.cs.tsukuba.ac.jp).

Manuscript received xx xx, 2013; revised xx xx, 2013.

[1]Unless otherwise specified, the channels mentioned hereafter in this paper refer to licensed spectrum bands.

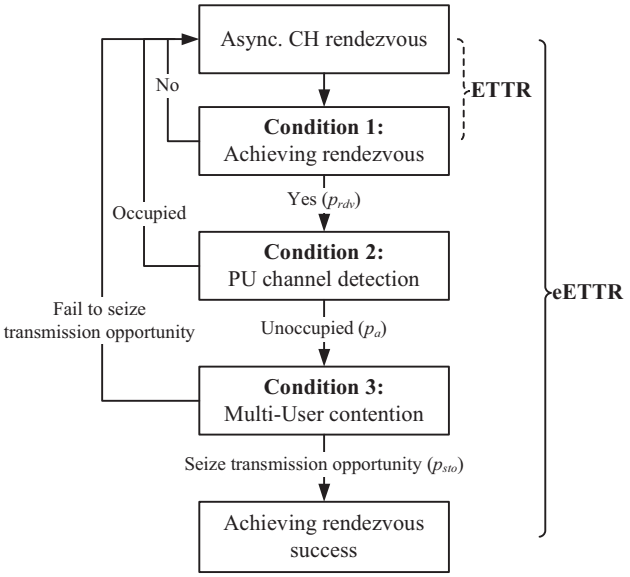

Fig. 1. Three conditions of achieving rendezvous success in asynchronous CH rendezvous based multi-user CRNs. The symbols in the parentheses are the corresponding probabilities in each hop slot.

the assistance of operation synchronization, that is, all SUs start rendezvous process simultaneously at the beginning of their respective CHSs. However, operation synchronization is difficult to reach in distributed CRNs. Hence, asynchronous CH rendezvous schemes (e.g., GOS [10], AMOCH [11], JS [12], CRSEQ [13], DRSEQ [14], and ETCH-ASYN [9]) are prevailing in the research on CH based rendezvous schemes. Researchers carefully construct CHSs with *rotation closure property* [11] to guarantee rendezvous within a finite time in the absence of operation synchronization.

To evaluate rendezvous delay performance of asynchronous CH rendezvous schemes, expected time-to-rendezvous (ETTR) is used as the main performance metric. However, ETTR in the literature is only relevant to the hopping pattern of a specifically designed CHS, and it is unable to reflect the channel access delay in the MAC layer. To study the channel access delay, we define a new metric, named effective ETTR (eETTR) in section II-B, to capture the aggregate effect of asynchronous CH rendezvous schemes, channel availability and the related MAC protocol. To better understand, two related concepts need to be differentiated.

- *Achieving rendezvous*: when a rendezvous pair jumps into a common channel (i.e., rendezvous channel) in the same hop slot[2] (i.e., rendezvous slot), they achieve rendezvous. Achieving rendezvous provides transmission opportunity (i.e., common media for transmission) to the rendezvous pair, which is completely dominated by the hopping patterns of CHSs generated by asynchronous CH rendezvous schemes. As ETTR is used to evaluate the delay of achieving rendezvous (see Fig.1), it only reflects the effect of asynchronous CH rendezvous schemes.
- *Achieving rendezvous success*: when a rendezvous pair achieves rendezvous and establishes a communication link successfully, they achieve rendezvous success. As shown in Fig.1, achieving rendezvous is a necessary but insufficient condition for achieving rendezvous success. Other necessary conditions include: (1) The transmission opportunity provided by asynchronous CH rendezvous schemes is available; (2) MAC functions, such as channel contention, probing receivers and performing handshaking process, help the rendezvous pair seize the transmission opportunity. eETTR is used to evaluate the delay of achieving rendezvous success, which reflects not only the effect of asynchronous CH rendezvous schemes but also the effect of channel availability and the MAC protocol.

[2]Each hop slot of a CHS is different from the backoff mini-slot of the 802.11 DCF in the following sections

Existing asynchronous CH rendezvous schemes target at single-radio multi-channel (SRMC) CRNs where each SU is equipped with a single hardware-constrained radio and works only on one channel at a time. To the best of our knowledge, how to integrate 802.11 DCF based CSMA/CA MAC with these asynchronous CH rendezvous schemes to coordinate multi-user contention has not been researched so far. The performances of SRMC CRNs based on asynchronous CH rendezvous schemes are analyzed in [15], [16] and [17], but they employ the S-ALOHA MAC. In [18], [19] and [20], 802.11 CSMA/CA MAC is introduced for channel access. However, their considered CRNs are single-radio single-channel (SRSC) CRNs where rendezvous problem does not exist. The research work [21], [22] and [23] study CSMA/CA MAC for SRMC CRNs, but the considered SRMC CRNs are reduced to SRSC CRNs by equipping each SU with a full-spectrum radio. Some existing asynchronous CH rendezvous schemes [8], [11], [12] have mentioned that 802.11 CSMA/CA MAC is used for channel access, but not present the details.

The contributions of this paper are summarized as follows.

- We analyze the channel access delay performance by integrating a modified Bianchi model [24] and an Absorbing Markov Chain model [25], which captures the aggregate effect of asynchronous CH rendezvous schemes, channel availability, and the MAC protocol.
- We tailor the 802.11 DCF to work appropriately with existing asynchronous CH rendezvous schemes. Redesigned mechanisms of 802.11 DCF include: (1) Amending backoff counter control for the slotted operation manner of existing asynchronous CH rendezvous schemes; (2) Enhancing the traditional virtual carrier sensing (VCS) mechanism to alleviate the impact of false collision problem on channel access delay performance.

The rest of this paper is organized as follows. The system model and the concerned performance metrics are explained in Section II, where the expression of eETTR is formulated. Following that, the details of the tailored 802.11 DCF are presented in Section III. To derive eETTR, the rendezvous statistics of existing asynchronous CH rendezvous schemes and the behavior of MAC protocol are analyzed in Section IV and Section V, respectively. In Section VI, the analytical results are verified through extensive simulations. Finally, the paper is concluded in Section VII.

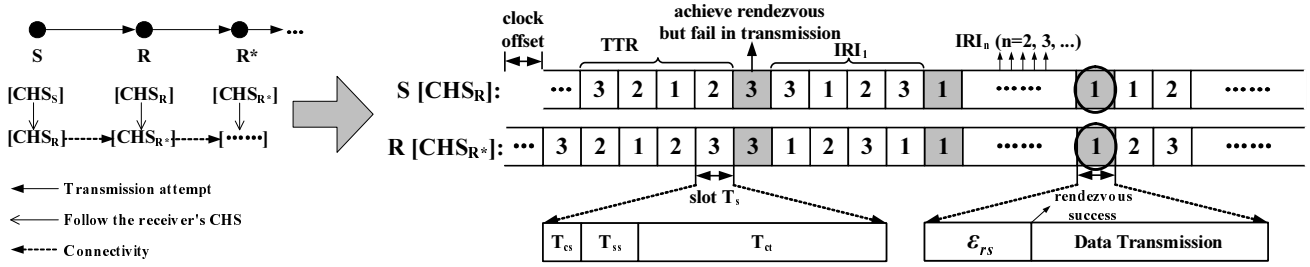

Fig. 2. The process of achieving rendezvous success (e.g., the GOS scheme [10]). The logical partition problem is illustrated in the leftmost part. Sender S follows the CHS of the receiver R for transmission, while the R has followed the CHS of its receiver R*. Then S and R can not always achieve rendezvous and the logical partition problem happens. In the rightmost part, all the gray blocks (with or without circle) denote that S and R achieve rendezvous. Due to PU activity or multi-user contention, the rendezvous pair may encounter rendezvous failure (gray blocks without circle). The rendezvous process proceeds till they finally achieve rendezvous success (the gray block with circle). TTR denotes the slots the rendezvous pair takes to achieve the first rendezvous, and IRI_n denotes the slots they have to take to achieve the next rendezvous when having encountered n consecutive rendezvous failures.

II. System Model and Preliminaries

A. Network Model

We consider a distributed CRN where all SUs are located in a single contention domain and have the same channel set with N orthogonal channels labeled as $1, 2, \cdots, N$. All these N channels are licensed to a primary network where PUs communicate with each other in a synchronous slotted manner. Each SU is equipped with a single half-duplex radio, which only works on a channel at a time but can switch among these *N* channels. As it is time-consuming for a SU to sense all the channels by using a single radio and the sensed available channels will become invalid during rendezvous process due to dynamic channel availability, SUs use all the N channels but not the sensed available channels to construct their CHSs. To this end, the CHSs are constructed by using asynchronous CH rendezvous schemes designed under symmetric model [7]. All SUs are in saturated transmission state and each SU randomly chooses a neighbor as its receiver for each transmission. In this fully loaded generic CRN [26], the *logical partition* problem [27] becomes most serious so that the connectivity between SUs is sustained by the rendezvous capability of the employed asynchronous CH rendezvous scheme (see Fig.2), but it can help us clarify the difference between ETTR and eETTR.

As all SUs are not synchronized in an asynchronous network setup, the overlapping duration T_o of slots between any two CHSs should be long enough to support a successful transmission, which suggests each slot duration T_s be $2T_o$ at least. In this sense, the asynchronous CH rendezvous system is equivalent to its slot-aligned counterpart with slot duration $T_s = T_o$ [12]. For analytical simplicity, we assume the clock offset between any two SUs is random integer multiple[3] of slot duration (see Fig.2), and the related analytical results under this assumption can be regarded as the optimal values of those under arbitrary clock offset. Each slot duration T_s is constituted by three parts (see Fig.2): channel switch overhead T_{cs}, spectrum sensing period T_{ss} and contention-transmission period T_{ct}. As the channel switch overhead is of microseconds [29] and the duration of a slot is of milliseconds in related standards (e.g., $10ms$ in IEEE 802.22 [30]), we assume channel switch overhead is negligible. After hopping into a channel, each SU performs spectrum sensing for a fixed time T_{ss} on the current channel and decides whether to access this channel according to the local sensing outcome. When SUs find the channel is not occupied by PUs in current slot, they try to establish communication links by using 802.11 DCF.

Channel availability of the CRN is subjected to PU activity. We employ the widely used ON-OFF markov chain model [28] [31] to formulate the PU activity in each channel, from which the steady-state probability p_a of channel availability in each hop slot is derived (see (1) in [31]). We assume the spectrum sensing result of each SU is perfect, which conforms to that in existing work on asynchronous CH rendezvous schemes for fair comparison in the following sections. Certainly, our analysis can be easily extended for imperfect spectrum sensing. The performance of imperfect spectrum sensing can be characterized by Receiver Operation Characteristic (ROC) curve which expresses the relationship between the false alarm probability ϵ and the miss detection probability ζ. According to the separation principle in [28], we can choose a operation point (ϵ^*, ζ^*) from the ROC curve to not violate the interference tolerance of PUs. Thus, probability of channel availability perceived by SUs is expressed as $p_a' = (1-\epsilon^*)p_a + \zeta^*(1-p_a)$, which can be used for our analysis under imperfect spectrum sensing. As ϵ^* and ζ^* are functions of spectrum sensing period T_{ss}[4] (see (18) and (19) in [28]), we can determine T_{ss} when giving (ϵ^*, ζ^*) and incorporate it into the analytical result under perfect spectrum sensing. As spectrum sensing performance does not belong to network factors which make channel access delay different from rendezvous delay, we do not consider the impact of imperfect spectrum sensing here.

B. Performance Metrics

By assuming that achieving rendezvous is equivalent to achieving rendezvous success in the literature, ETTR is applicable to evaluating channel access delay. Actually, it is not the case. There are two network factors (i.e., condition 2 and 3 in Fig.1) that may convert achieving rendezvous into *achieving rendezvous failure*: (1) The rendezvous channel is unavailable

[3]This goal can be achieved by referring to the slot information broadcast by the primary network [28]

[4]Spectrum sensing period T_{ss} is the product of the sampling rate and the number of samples

due to PU activity; (2) The rendezvous pair does not seize the transmission opportunity as they fail in competition for channel access due to multi-user contention. Thus, we propose two new metrics to assist in analyzing the channel access delay in multi-user SRMC CRNs based on asynchronous CH rendezvous schemes and CSMA/CA MAC.

1) Probability of seizing transmission opportunity (p_{sto}): When a rendezvous pair achieves rendezvous over an *available* channel, they may fail to seize this transmission opportunity due to multi-user contention. The p_{sto} is introduced to capture the impact of multi-user contention on channel access delay. Obviously, high p_{sto} indicates high time-efficiency in communication link establishment. To increase p_{sto}, a sender needs to be provided with more number of rendezvous attempts (i.e., probing its intended receiver) in the duration-limited rendezvous slot, which relies on the collision avoidance mechanism of the CSMA/CA MAC.

2) Effective expected time to rendezvous (eETTR): In the literature, ETTR is used to evaluate the average delay of the *first* rendezvous achievement (see Fig.2), while the proposed metric eETTR accounts for the average delay to achieve rendezvous success which contains multiple rendezvous achievements. When a sender wants to communicate with its intended receiver, it costs TTR slots to achieve the first rendezvous. In the rendezvous slot, the rendezvous pair has probability $p_a p_{sto}$ to achieve rendezvous success. Once they fail to achieve rendezvous success, the rendezvous pair has to cost extra $1 + IRI$ slots to achieve the next rendezvous. IRI is the abbreviation of inter-rendezvous interval. In a long run, the rendezvous pair undergoes $\frac{1}{p_a p_{sto}} - 1$ rendezvous failures on average and suffers penalty of $1 + EIRI$ slots on average for each rendezvous failure. EIRI denotes the average value of IRI. When the rendezvous pair finally achieves rendezvous success (see Fig.2), a portion of the rendezvous slot ε_{rs} is used as the control overhead to establish a communication link, of which the average value is denoted by $\overline{\varepsilon_{rs}}$. Thus, we write the expression of eETTR as below

$$\begin{aligned} eETTR =& ETTR + \frac{(1 - p_a p_{sto})(1 + EIRI)}{p_a p_{sto}} \\ &+ \overline{\varepsilon_{rs}} \quad (\text{in slot}). \end{aligned} \tag{1}$$

where ETTR and EIRI are dominated by rendezvous patterns of asynchronous CH rendezvous schemes, p_a is determined by PU activity, and p_{sto}, as well as $\overline{\varepsilon_{rs}}$, relates to MAC protocol. Obviously, the metric eETTR captures the aggregate effect of asynchronous CH rendezvous schemes, channel availability and MAC protocol on channel access delay. To derive eETTR, we analyze ETTR and EIRI in Section IV and obtain p_{sto} and $\overline{\varepsilon_{rs}}$ in Section V.

III. Tailored 802.11 DCF for Asynchronous CH Rendezvous

As random access is well suited to distributed wireless networks, we integrate 802.11 DCF based CSMA/CA MAC with existing asynchronous CH rendezvous schemes to coordinate multi-user contention. However, to provide a reasonable evaluation of channel access delay, the mismatch between 802.11 DCF and asynchronous CH rendezvous schemes needs to be eliminated first. For concise presentation, the refined 802.11 CSMA/CA MAC is named CH-CSMA/CA MAC hereafter.

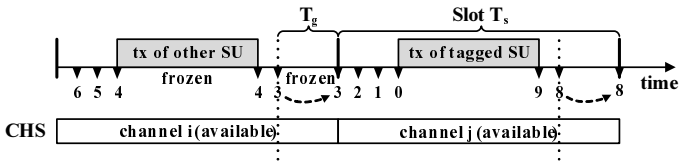

Fig. 3. The control of backoff counter in CH-CSMA/CA MAC

A. Channel Access Scheme

Before data transmission, SUs have to detect whether they have achieved rendezvous with their respective receivers by sending probing packets for rendezvous attempts. To this end, we use RTS/CTS packets as the probing packets to reduce waste of bandwidth, and RTS/CTS access scheme is mandatory in CH-CSMA/CA MAC. Once a rendezvous pair achieves rendezvous success, all the remaining time of the rendezvous slot is used for transmission with packet aggregation, as this policy can improve channel utilization efficiency.

B. Amended Control of Backoff Counter

The control of backoff counter is the key function of 802.11 DCF to support random access and collision avoidance. When a tagged SU (i.e., a SU selected arbitrarily) has packets to transmit and its current sojourn channel is available and sensed idle for DIFS, the tagged SU selects a value randomly from $[0, CW_{min} - 1]$ to set its backoff counter and enters the backoff counting-down process. CW_{min} denotes the minimum size of the contention window. During backoff counting-down process, the backoff counter is decremented by one, provided that the channel keeps idle for a backoff mini-slot with duration $\sigma\mu s$. Once the channel becomes busy, the backoff counter is frozen. It is activated as long as the channel changes into idle again for DIFS. When the backoff counter reaches zero, the tagged SU transmits a RTS packet for rendezvous attempt and waits for the replied CTS packet. In the case of failing to receive the desired CTS packet, the tagged SU deems that the transmitted RTS packet is corrupted by collision and it doubles its contention window size to $W_i = 2^i CW_{min}$ where $W_0 = CW_{min}$ and i denotes the number of collisions the tagged SU encounters. The contention window size remains at $W_i = W_m = 2^m CW_{min}$ when $i > m$. W_m is the maximum contention window size and m is the maximum backoff stage. After sending the data packet successfully, the tagged SU resets the contention window size to CW_{min}.

What explained above is the conventional control of backoff counter, in which backoff counter is only frozen when the channel becomes busy. To integrate 802.11 DCF with asynchronous CH rendezvous schemes, the backoff counter frozen mechanism needs to be refined to protect PUs from harmful interference and packets from truncation:

- In order to avoid interference with PUs, the tagged SU has to freeze its backoff counter for the whole slot duration

when its sojourn channel is occupied by PUs. Otherwise, the tagged SU may transmit concurrently with the PU when it backoff counter reaches zero. At the beginning of the next slot, the tagged SU resumes its backoff counter if the channel it switches into is available and sensed idle for DIFS.

- To avoid packet truncation due to the slotted operation manner of existing asynchronous CH rendezvous schemes, the tagged SU needs to freeze its backoff counter till the end of current slot if the remaining time of the slot is less than T_g (see Fig.3). T_g in (2) equals the time required for the complete transmission of a data packet, which performs as a guard time to protect the integrity of each packet transmission.

$$T_g = t_{rts} + 3SIFS + t_{cts} + t_{data} + t_{ack}. \quad (2)$$

where t_{rts}, t_{cts}, t_{data} and t_{ack} denote the transmission time of RTS, CTS, DATA and ACK packets, respectively.

C. Enhanced Virtual Carrier Sensing (EVCS)

Most 802.11 packets have a *duration* field and use it to reserve channel by notifying neighbors the channel busy duration. To reach this goal, the virtual carrier sensing (VCS) [32] is realized by a timer named network allocation vector (NAV) which is assigned the value in the duration field of the overheard packet. When packets arrive, MAC protocols need first check whether NAV is zero or not. Although VCS estimates the channel busy duration well in conventional wireless networks, it causes inconsistency problem between the actual channel busy duration and the NAV value due to the identified ***false collision***. Consider a single-hop CRN as shown in Fig.4. When SU S wants to communicate with SU R, it sends a RTS packet for rendezvous attempt. In the RTS duration field, the value t_{vcs}^{rts} in (3) is used to reserve the channel for the subsequent data transmission. However, two types of collisions will cause RTS transmission failure.

$$t_{vcs}^{rts} = 3SIFS + t_{cts} + t_{data} + t_{ack}. \quad (3)$$

- *True collision*. It happens when the RTS packet sent from SU S is corrupted by other RTS packets sent at the same time. As neighboring SUs (e.g., r_1 and r_2) on the same channel of SU S can not extract the value t_{vcs}^{rts} in the corrupted RTS packet, they will not set their NAV timer and freeze their backoff counters. In this case, the channel busy time-inconsistency problem does not occur.
- *False collision*. It happens when SU S sends the RTS packet without true collision but SU R does not receive it, as they fail to achieve rendezvous. Since neighboring SUs (e.g., r_1 and r_2) on the same channel of SU S can extract the value t_{vcs}^{rts} in the received RTS packet, they will freeze their backoff counters for t_{vcs}^{rts}, while the channel is not busy for t_{vcs}^{rts} actually (see in Fig.4). In this case, the channel busy time-inconsistency problem emerges and SU r_1 and SU r_2 have to suffer extra delay t_{vcs}^{rts}.

It is worth noting that false collision problem may also emerge in conventional wireless networks with error-prone channel. In practice, this problem is suppressed by transmitting the control packets at basic PHY rate. However, Even with the ideal channel condition, the CH-CSMA/CA MAC still encounters the false collision problem.

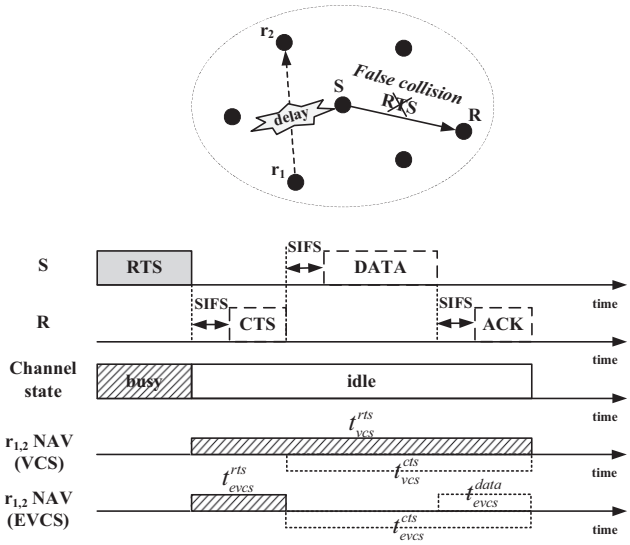

Fig. 4. Channel busy time-inconsistency problem due to false collision. For the rendezvous pair SU S and SU R, the subsequent transmission of CTS, DATA and ACK will not be carried out when false collision happens. However, the rendezvous pair r_1 and r_2 still believe that the channel remains busy after overhearing the RTS sent from SU S. Consequently, extra delay is injected into their backoff process. The extra injected delay under VCS and EVCS are denoted by blocks with slopping lines.

The fundamental cause of channel busy time-inconsistency problem is that VCS is designed for the scenario where the senders can always achieve rendezvous with their receivers. Actually, a rendezvous pair can not always achieve rendezvous by relying on existing asynchronous CH rendezvous schemes. The channel busy time-inconsistency problem is very detrimental to channel access delay. Assume that SU r_1 and SU r_2 have achieved rendezvous on the same channel of SU S, and SU r_1 enters the backoff counting-down process for communication with SU r_2 (see Fig.4). Suppose that SU S transmits a RTS packet, prior to SU r_1, to its receiver SU R and encounters false collision. After overhearing the RTS packet sent from SU S, SU r_1 freezes its backoff counter and sets its NAV to t_{vcs}^{rts}. Consequently, SU r_1 has to suffer extra delay of t_{vcs}^{rts} before attempting rendezvous with SU r_2. As the channel busy time-inconsistency problem may happen in each backoff counting-down action, SU r_1 will suffer severe cumulative delay for each rendezvous attempt. Recall that each slot is duration-limited, the extra delay injected into backoff counting-down process will reduce the number of rendezvous attempts in the rendezvous slot and decrease the probability of seizing transmission opportunity for rendezvous pairs. Therefore, solving the channel busy time-inconsistency problem is important to improve channel access delay.

To alleviate the negative impact of channel busy time-inconsistency problem on channel access delay, we propose an enhanced virtual carrier sensing (EVCS) which is simple but effective. The EVCS mechanism works like VCS mechanism in the data fragmentation burst scenario where the value in the duration field of each data fragment only reserves the

TABLE I
TABLE OF NOTATIONS

Symbols	Explanations
N	The total channel number in the CRN
T	The period duration of the CHS designed in a specific asynchronous CH rendezvous scheme
Γ, Δ	The absolute and effective clock offset between two SUs
$ETTR$	The average slots to achieve the first rendezvous
$EIRI$	The average slots between two successive events of achieving rendezvous
$eETTR$	The average delay of channel access
p_a	The perceived probability of channel availability
n	SU density per channel in each hop slot
τ	The transmission probability for a SU
p_{tc}, p_{fc}	The probability of true collision and false collision encountered by a SU
$\widehat{T}_{tc}$, $\widehat{T}_{fc}$	The time overhead when a SU encounters true collision and false collision
p_c	The probability of collision encountered by a SU
p_s	The probability of transmitting RTS without true collision
p_{rdv}	Rendezvous probability in each hop slot
$\widehat{p}_s$, $\widehat{p}_f$	The probability of achieving and failing to achieve rendezvous success between two successive backoff actions for a SU when it achieves rendezvous
p_{sto}	The probability of achieving rendezvous success for a SU when it achieves rendezvous on an available channel

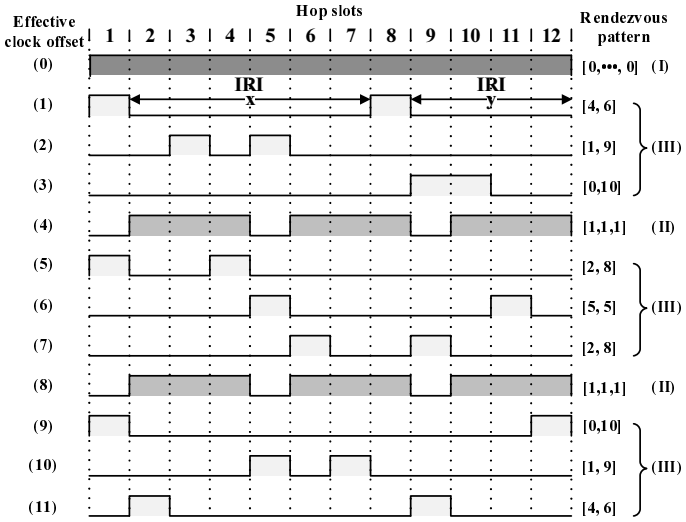

Fig. 5. Rendezvous patterns of the GOS scheme (when $N = 3$). The values included in a square bracket are the elements of a tuple, which is used to represent a rendezvous pattern under a specific effective clock offset. Each of the value denotes the duration of a IRI in the rendezvous pattern.

channel for the transmission of the subsequent data fragment. Suppose SU S and SU R have achieved rendezvous, and SU R receives the RTS packet from SU S successfully. In EVCS (see Fig.4), the value t_{evcs}^{rts} in (4) only contains the transmission time of the next CTS packet, but the transmission time of next DATA and ACK packets are not contained. SU R replies CTS packet which has duration field with value $t_{evcs}^{cts} = t_{vcs}^{cts} = 2SIFS + t_{data} + t_{ack}$ for the next transmission of DATA and ACK packets. After receiving the replied CTS packet, SU S and SU R set the value in the duration field of their respective DATA and ACK packets according to the DATA packet size as follows.

$$t_{evcs}^{rts} = SIFS + t_{cts}. \tag{4}$$

- When the size of DATA packet does not exceed the maximum MAC Service Data Unit (MSDU), SU S sends the DATA packet with duration value $t_{evcs}^{data} = SIFS + t_{ack}$ equal to the transmission time of ACK from SU R, and SU R replies ACK with duration value $t_{evcs}^{ack} = 0$ by checking that more fragments flag in the frame control filed of the received DATA packet is zero.
- Otherwise, SU S sends a DATA fragment with duration value $t_{evcs}^{data} = 3SIFS + t_{data} + 2t_{ack}$ equal to the transmission time of current ACK and the subsequent DATA fragment and ACK. SU R replies ACK with duration value $t_{evcs}^{ack} = 2SIFS + t_{data} + t_{ack}$ by checking that more fragments flag in the frame control filed of the received DATA fragment is one.

Once false collision occurs, the SU victims under EVCS suffer extra delay t_{evcs}^{rts} which is much less than t_{vcs}^{rts}. As the delay injected into backoff counting-down process is reduced, a rendezvous pair can carry out more rendezvous attempts in their rendezvous slots to increase the probability of seizing transmission opportunity. Therefore, the channel access delay performance under EVCS is better than that under VCS.

IV. RENDEZVOUS STATISTICS OF ASYNCHRONOUS CH RENDEZVOUS SCHEMES

Rendezvous statistics denoted by ETTR and EIRI are completely dominated by the designed CHSs of existing asynchronous CH rendezvous schemes. To derive eETTR, we need first obtain these two parameters from their rendezvous patterns (i.e., patterns of achieving rendezvous). The main notations used in analysis are listed in Table I.

The common feature of CHSs designed in asynchronous CH rendezvous schemes is ***periodicity***, and a subsequence pattern with a period duration repeats during rendezvous process. Given the clock offset between a rendezvous pair, a rendezvous pattern also repeats during rendezvous process (see Fig.5). Due to space constraint, we take the seminal work GOS scheme [10] as an example for analysis of rendezvous statistics. Other asynchronous CH rendezvous schemes can be analyzed by referring to this example.

In the GOS scheme, the period duration T of the proposed CHS is of $N(N+1)$ slots. Due to periodicity, the rendezvous patterns under *absolute* clock offset $\Gamma \in \{0, 1, \cdots\}$ are the same as those under *effective* clock offset $\Delta = \Gamma \ mod \ T$ and $\Delta \in [0, 1, \cdots, T-1]$. Suppose $N = 3$ and a channel permutation is {1,2,3}, then we get a subsequence pattern {**1**,1,2,3,**2**,1,2,3,**3**,1,2,3} which is also a period of the CHS (see Fig.2 and refer to [10] for the details of CHS construction). By changing Δ from 0 to $T-1$, we get the corresponding rendezvous patterns as shown in Fig.5. Each square protrusion in Fig.5 denotes that a rendezvous pair has achieved rendezvous. We use tuples (a data structure where elements are organized in a square bracket) to express these rendezvous patterns and all elements of a tuple are the durations of IRIs in a period of a specific rendezvous pattern. For the GOS scheme, there exist three types of rendezvous patterns (marked by shadows with three different gray levels in Fig.5), and their occurrence conditions and probabilities are listed in Table II.

$$\begin{aligned} ETTR_{III} &= \frac{1}{N^2}\sum_{x\in\{0,1,\cdots N(N+1)-2\}\backslash\{x^*\}}\frac{1}{N(N+1)}[0+0+(1+2+\cdots+x)+(1+2+\cdots+y)] \\ &= \frac{1}{N^2}\sum_{x\in\{0,1,\cdots N(N+1)-2\}\backslash\{x^*\}}\frac{1}{2N(N+1)}(x+y+x^2+y^2) \\ &= \frac{1}{2N^3(N+1)}\sum_{x\in\{0,1,\cdots N(N+1)-2\}\backslash\{x^*\}}(x^2-2\mathcal{C}x+\mathcal{C}^2+\mathcal{C}) \quad (\text{where } \mathcal{C}=x+y=N(N+1)-2) \quad (\text{in slot}). \end{aligned} \tag{7}$$

TABLE II
OCCURRENCE CONDITIONS AND PROBABILITIES OF RENDEZVOUS PATTERNS IN GOS SCHEME

rendezvous pattern	condition and probability
(I) $\underbrace{[0,0,\cdots 0]}_{N(N+1)}$	when $\Delta = 0$. This type of rendezvous pattern occurs only once in the total $N(N+1)$ rendezvous patterns, then the probability p_I is $\frac{1}{N(N+1)}$.
(II) $\underbrace{[1,1,\cdots 1]}_{N}$	when Δ is integer multiple of $N+1$. This type of rendezvous patterns occurs $N-1$ times in the total $N(N+1)$ rendezvous patterns, then the probability p_{II} is $\frac{N-1}{N(N+1)}$.
(III) $[x,y]$	when Δ are other cases. This type of rendezvous pattern occurs N^2 times in the total $N(N+1)$ rendezvous patterns, then the probability p_{III} is $\frac{N^2}{N(N+1)}$.

A. Expected time to rendezvous (ETTR)

In the GOS scheme, ETTR is calculated on condition that a sender starts rendezvous at the initial position of its own CHS. However, when the sender attempts transmission, it will start rendezvous at any position of its followed CHS. For this reason, we need to recalculate ETTR of the GOS scheme. Due to the three types of rendezvous patterns (see Table II), the derivation of ETTR is conducted in three parts.

For rendezvous pattern (I), there are no IRIs in a period, so we write the ETTR of this type as

$$ETTR_I = 0 \quad (\text{in slot}). \tag{5}$$

For rendezvous pattern (II), there are N IRIs in a period. As each has duration of one slot, we therefore get

$$ETTR_{II} = \frac{N}{N(N+1)} = \frac{1}{N+1} \quad (\text{in slot}). \tag{6}$$

For rendezvous pattern (III), there are two IRIs with total duration of $T-2$ slots in a period, as the GOS scheme can only guarantee two rendezvous slots in a period under this type of rendezvous pattern. we use tuples $[x,y]$ to describe this type of rendezvous patterns where $x+y = T-2 = N(N+1)-2$. As a sender will start rendezvous at an arbitrary position of its own CHS when it has packets to transmit, either of these two rendezvous slots and any slot in these two IRIs (with duration x and y slots) may be taken as the starting position of rendezvous. We write $ETTR_{III}$ in (7). From (7), the order of x and y in the tuple has no effect on the ultimate result of $ETTR_{III}$, hence $[x,y]$ is equivalent to $[x',y']$ when $x = x'$ and $y = y'$ or $x = y'$ and $y = x'$, and the the range of x can be compressed to range $\{0,1,\cdots,\frac{N(N+1)}{2}-1\}\backslash\{x^*\}$. Since the sum of x and y is a constant when N is fixed, we use tuple $[x]$ with only one element to represent each rendezvous pattern of this type. $\{x^*\}$ denotes the numbers that x is unable to be assigned. For example, in Fig.5, $\{x^*\} = \{3\}$ as the rendezvous pattern $[3,7]$ does not appear. By excluding these invalid rendezvous patterns, we get the final $ETTR_{III}$ expression derived from (7) in two cases.

When N is odd, we write

$$ETTR_{III} = \frac{2(\sum_{\Theta} A) - A\Big|_{x=\frac{N(N+1)}{2}-1}}{2N^3(N+1)} \quad (\text{in slot}). \tag{8}$$

When N is even, we write

$$ETTR_{III} = \frac{\sum_{\Theta} A}{N^3(N+1)} \quad (\text{in slot}). \tag{9}$$

In (8) and (9), Θ denotes $x \in \{0,1,\cdots,\frac{N(N+1)}{2}-1\}\backslash\{x^*\}$, where $\{x^*|N+(\kappa-1)(N+1), \kappa \in \{1,2,\cdots,\lfloor\frac{N}{2}\rfloor\}\}$ (related details are presented in appendix A), and $A = (x^2-2\mathcal{C}x+\mathcal{C}^2+\mathcal{C})$. $A\Big|_{x=\frac{N(N+1)}{2}-1}$ is the value of A when $x = \frac{N(N+1)}{2}-1$. Finally, by combining (5), (6) and (7), we get

$$ETTR = p_I ETTR_I + p_{II} ETTR_{II} + p_{III} ETTR_{III} \text{ (in slot)}. \tag{10}$$

B. Expected inter-rendezvous interval (EIRI)

EIRI is employed to evaluate the average time overhead for a rendezvous pair to achieve the next rendezvous when they encounter rendezvous failure. As the derivation of EIRI is on the precondition that a rendezvous pair fail to achieve rendezvous success in current rendezvous slot, it is different from the derivation of ETTR. The derivation of EIRI is also conducted in three parts.

For rendezvous pattern (I), as there are no IRIs, we write the EIRI of this type as

$$EIRI_I = 0 \quad (\text{in slot}). \tag{11}$$

For rendezvous pattern (II), there are N IRIs (each has one slot duration) and $N(N+1)-N$ rendezvous slots in a period. Then, we get the EIRI of this type

$$EIRI_{II} = \frac{N}{N(N+1)-N} = \frac{1}{N} \quad (\text{in slot}). \tag{12}$$

For rendezvous pattern (III), a period has two IRIs with total duration of $N(N+1)-2$ slots and two rendezvous slots, then

$$\begin{aligned} EIRI_{III} &= \frac{N(N+1)-2}{N(N+1)-(N(N+1)-2)} \\ &= \frac{N(N+1)}{2}-1 \quad (\text{in slot}). \end{aligned} \tag{13}$$

Finally, by combining (11), (12) and (13), we get

$$\begin{aligned} EIRI &= p_I EIRI_I + p_{II} EIRI_{II} + p_{III} EIRI_{III} \\ &= \frac{N-1}{N(N+1)}\frac{1}{N} + \frac{N^2}{N(N+1)}(\frac{N(N+1)}{2} - 1) \\ &= \frac{N^2}{2} + \frac{1}{N^2} - \frac{N^3+2}{N^2(N+1)} \quad \text{(in slot)}. \end{aligned} \tag{14}$$

When $N = 1$, $EIRI = 0$ is expected in (14).

V. Numerical Analysis of Channel Access Delay

In this section, we employ a modified Bianchi model to get two key parameters (i.e., transmission probability and collision probability) required in analysis of channel access delay and an Absorbing Markov Chain model to obtain p_{sto} and $\overline{\varepsilon_{rs}}$.

A. Key Parameters

As backoff counting-down processes of all SUs are homogeneous [19], the transmission probability τ of a tagged SU can be obtained by directly using the Bianchi model as below (see (7) in [24])

$$\tau = \frac{2(1-2p_c)}{(1-2p_c)(W_0+1) + p_c W_0(1-(2p_c)^m)}. \tag{15}$$

In Bianchi model, p_c means the probability of collision which only contains true collision, while collision in the CH-CSMA/CA MAC contains true collision and false collision. Thus, we need modify the derivation of collision probability. Firstly, we get the probability of true collision

$$p_{tc} = 1 - (1-\tau)^{n-1}. \tag{16}$$

The parameter n in (16) denotes the SU density per channel in each slot. In order to guarantee access fairness for each channel, the appearance frequency of all channels are identical in a period of CHSs generated in existing asynchronous CH rendezvous schemes. As the clock offset between any two SUs is purely random, the SU density per channel can be assumed identical in each slot. Then we get $n = \frac{M}{N}$ when the total number of SUs is M. False collision emerges when the tagged SU transmits successfully but fails to achieve rendezvous with its intended receiver. The probability p_s that the tagged SU transmits successfully is

$$p_s = (1-\tau)^{n-1}. \tag{17}$$

The tagged SU achieves the first rendezvous with its intended receiver at cost of $ETTR$ slots and takes additional $EIRI + 1$ slots to achieve each subsequent rendezvous when encountering rendezvous failure. By considering the steady-state of this process, we use the reciprocal of $EIRI + 1$ in (18) to approximate the probability of achieving rendezvous p_{rdv} in each slot for the tagged SU as $ETTR$ and $EIRI$ are of the same order of magnitude $O(N^2)$.

$$p_{rdv} = \frac{1}{EIRI + 1}. \tag{18}$$

From (17) and (18), we get the probability of false collision

$$p_{fc} = p_s(1 - p_{rdv}). \tag{19}$$

As true collision and false collision are mutual exclusive events, we get p_c by combining (16) and (19)

$$\begin{aligned} p_c &= p_{tc} + p_{fc} \\ &= 1 - (1-\tau)^{n-1} + (1 - \frac{1}{EIRI+1})(1-\tau)^{n-1} \\ &= 1 - \frac{1}{EIRI+1}(1-\tau)^{n-1}. \end{aligned} \tag{20}$$

When $EIRI \to 0$, we get $p_{rdv} \to 1$ and $p_c \to p_{tc}$, which indicates that the parameter p_c has the same meaning as that in Bianchi model when SUs can always achieve rendezvous with their respective intended receivers. The results of τ and p_c can be obtained by solving (15) and (20) jointly through numerical methods.

B. Analysis of Seizing Transmission Opportunity

By subdividing each slot into K backoff mini-slots to construct a discrete time system, we label all K backoff mini-slots of a hop slot as $0, 1, \cdots, K-1$ and employ the Absorbing Markov Chain (AMC) theory [25] to calculate the probability p_{sto} of the tagged SU in one of its rendezvous slots. By removing the guard time T_g at the end of the rendezvous slot, the effective time for attempting transmission is $T_s - T_g + \sigma$, i.e., $K - K_g + 1$ backoff mini-slots where K_g equals the conversion of guard time T_g into unit of backoff mini-slot. We call this rendezvous slot the 'concerned slot' hereafter.

During the probing process of the tagged SU in the concerned slot, it will encounter an idle, true or false collision event in each virtual mini-slot[5] with duration $\widehat{T}_i$, $\widehat{T}_{tc}$ and $\widehat{T}_{fc}$ and fall into two final states: (1) Seizing this transmission opportunity to establish a communication link, which is denoted as 'S'; (2) Failing to seize this transmission opportunity, which is denoted as 'F'. We treat these two final states as two absorbing states and formulate this probing process as a AMC model $\{\overrightarrow{\Omega}_k : 0 \le k \le K - K_g\}$, which has $K - K_g + 1$ transient states and two absorbing states in $\{0, 1, \cdots, K - K_g, S, F\}$ (see Fig.6). Each transient state denotes the index of a backoff mini-slot.

As SU density per channel in each slot is n, there are other $n-1$ non-tagged SUs on the same channel of the tagged SU. Note that, in the concerned slot, the tagged SU has achieved rendezvous with its intended receiver, while the other $n-1$ non-tagged SUs achieve rendezvous with their respective receivers with probability p_{rdv}. Therefore, false collision events can not be triggered by the tagged SU. By using the key parameters derived in section V-A, we write the probabilities $\widehat{p}_i$, $\widehat{p}_{tc}$ and $\widehat{p}_{fc}$ for idle, true collision and false collision events encountered by the tagged SU in each backoff mini-slot. These event durations are presented in (21) where

[5]Virtual mini-slot is the time between two successive backoff counting-down actions, which varies when the tagged SU encounters idle, true collision and false collision events

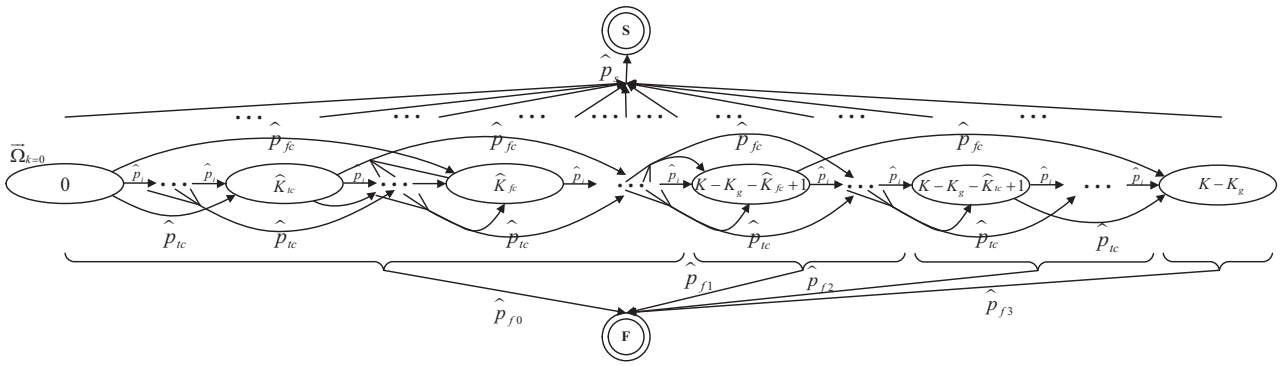

Fig. 6. State transition diagram of the AMC model. The ellipses denote transient states and the two annuluses denote the two absorbing states.

'w.p.' is the abbreviation for 'with probability'.

$$\begin{aligned}
&\widehat{T}_i = \sigma, \text{ w.p. } \widehat{p}_i = (1-\tau)^n \\
&\widehat{T}_{tc}{=}t_{rts}{+}DIFS, \text{ w.p. } \widehat{p}_{tc}{=}1{-}\widehat{p}_i{-}n\tau(1{-}\tau)^{n-1} \\
&\widehat{T}_{fc} = t_{rts} + t_{vcs}^{rts} + DIFS \quad \text{(under VCS)} \\
&\quad = t_{rts} + t_{evcs}^{rts} + DIFS \quad \text{(under EVCS)}, \\
&\quad \text{w.p. } \widehat{p}_{fc} = (n-1)\tau(1-\tau)^{n-1}(1-p_{rdv}).
\end{aligned} \tag{21}$$

$$\widehat{p}_s = \tau(1-\tau)^{n-1}$$

$$\widehat{p}_f = \begin{cases}
\widehat{p}_{f0} = (n-1)\tau(1-\tau)^{n-1}p_{rdv}, \\
\text{when } U \in [0, K-K_g-\widehat{K}_{fc}] \\
\widehat{p}_{f1} = \widehat{p}_{f0} + \widehat{p}_{fc}, \\
\text{when } U \in (K{-}K_g{-}\widehat{K}_{fc}, K{-}K_g{-}\widehat{K}_{tc}] \\
\widehat{p}_{f2} = \widehat{p}_{f1} + \widehat{p}_{tc}, \\
\text{when } U \in (K{-}K_g{-}\widehat{K}_{tc}, K{-}K_g) \\
\widehat{p}_{f3} = 1 - \widehat{p}_s, \text{when } U = K-K_g
\end{cases} \tag{22}$$

In each backoff mini-slot $U \in [0, K-K_g]$, the tagged SU is possible to fall into two absorbing states 'S' and 'F'. When the tagged SU transmits a RTS packet without true collision in the U^{th} backoff mini-slot, it falls into absorbing state 'S' in the U^{th} backoff mini-slot and uses the remaining time $V = K-U$ of the concerned slot to transmit data packets (see Fig.7). Otherwise, when the remaining time of the concerned slot is not enough to accommodate the transmission of a data packet after the tagged SU encounters an idle, true or non-own false collision event in the U^{th} backoff mini-slot or any one of the other $n-1$ non-tagged SUs achieves rendezvous success, the tagged SU falls into absorbing state 'F' in the U^{th} backoff mini-slot. Let $\widehat{K}_i$, $\widehat{K}_{tc}$ and $\widehat{K}_{fc}$ be equal to the conversion of $\widehat{T}_i$, $\widehat{T}_{tc}$ and $\widehat{T}_{fc}$ into unit of backoff mini-slot. Then we get the probabilities $\widehat{p}_s$ and $\widehat{p}_f$ of the tagged SU falling into either of these two absorbing states 'S' and 'F' in each backoff mini-slot $U \in [0, K-K_g]$ in (22). By combining (21) and (22), we write the canonical form of one-step transition probability matrix **P** for the AMC model

$$\mathbf{P} = \begin{bmatrix} \mathbf{Q} & \mathbf{R} \\ \mathbf{0} & \mathbf{I} \end{bmatrix} \tag{23}$$

and the details are presented in Fig.8.

According to the AMC theory, we first derive the *fundamental matrix* **N** of the matrix **P**. The elements $(\mathbf{N})_{0j}$ of the

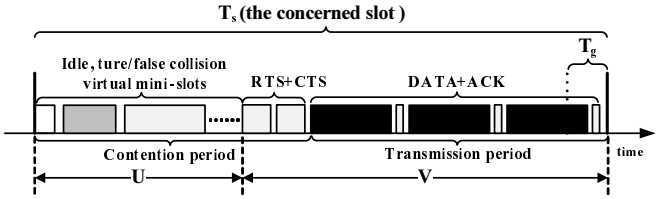

Fig. 7. Illustration of a successful transmission in the concerned slot.

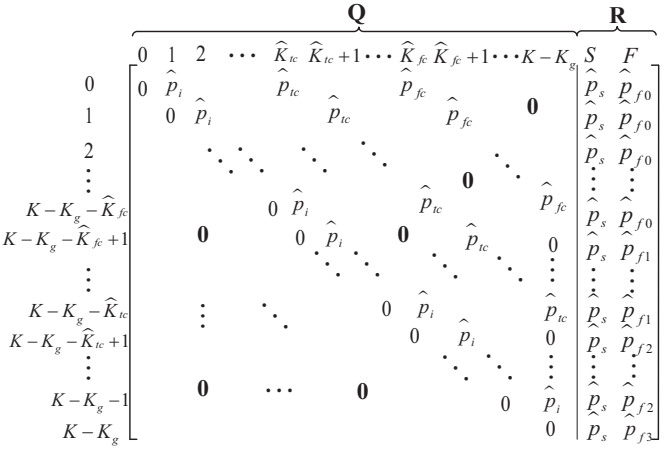

Fig. 8. The details of one-step transition probability matrix for AMC model

fundamental matrix **N** give the expected number of visits to a state $\overrightarrow{\Omega}_k = j$ $(0 \le j \le K-K_g)$ from the initial state $\overrightarrow{\Omega}_0 = 0$ for the tagged SU before being absorbed.

$$\begin{aligned}
(\mathbf{N})_{0j} &= \Big(\sum_{k=0}^{k=K-K_g} \mathbf{Q}^k\Big)_{0j} \qquad (0 \le j \le K-K_g) \\
&= ((\mathbf{I}{-}\mathbf{Q}^{K-K_g+1})(\mathbf{I}{-}\mathbf{Q})^{-1})_{0j}{=}((\mathbf{I}{-}\mathbf{Q})^{-1})_{0j}.
\end{aligned} \tag{24}$$

Note $(\cdot)_{ij}$ denotes the $(i,j)^{th}$ entry of a matrix. As sub-matrix **Q** is a $(K{-}K_g{+}1){\times}(K{-}K_g{+}1)$ *strict* upper triangular matrix, $\mathbf{Q}^k{=}\mathbf{0}$ when $k{\ge}K{-}K_g{+}1$ in (24). Assume the tagged SU reaches successful transmission in the j^{th} backoff mini-slot, and we denote this event as '$U{=}j$'. This event consists of three subevents: (i) The tagged SU does not fall into neither of the two absorbing states in any backoff mini-slot prior to the j^{th} backoff mini-slot, which is denoted by $\Upsilon_{U<j}^{\{S,F\}}{=}0$; (ii) The tagged SU visits the state $\overrightarrow{\Omega}_k{=}j$ from

the initial state $\overrightarrow{\Omega}_0$=0; (iii) The tagged SU reaches successful transmission in the state $\overrightarrow{\Omega}_k$=$j$, which is denoted by $\Upsilon_{U=j}^{\{S\}}$=1. Then, we get the probability p_{sto}^j of the event 'U=j'

$$\begin{aligned} p_{sto}^j &= \Pr\{U=j\} \\ &= \Pr\{\overrightarrow{\Omega}_k=j, \Upsilon_{U=j}^{\{S\}}=1 | \Upsilon_{U<j}^{\{S,F\}}=0, \overrightarrow{\Omega}_0=0\} \\ &= (\mathbf{N})_{0j}\widehat{p}_s \prod_{k=0}^{j-1}(1-(\mathbf{N})_{0k}(\widehat{p}_s+\widehat{p}_f)). \end{aligned} \quad (25)$$

For all $K-K_g+1$ backoff mini-slots in the effective time of the concerned slot, we write the probability of seizing this transmission opportunity p_{sto} for the tagged SU as below

$$p_{sto} = \sum_{j=0}^{K-K_g} p_{sto}^j. \quad (26)$$

C. Analysis of Channel Access Delay

As presented in (1), the last unknown parameter is $\overline{\varepsilon_{rs}}$. According to (25), we get the probability mass function of the random variable U which denotes the number of backoff mini-slots from the beginning of the concerned slot to the instant when a successful data transmission occurs. Then, we obtain its expected value

$$E(U) = \sum_{j=0}^{K-K_g} j p_{sto}^j. \quad (27)$$

As $\overline{\varepsilon_{rs}}$ denotes the ratio between $E(U)$ and the duration of the concerned slot, we write

$$\overline{\varepsilon_{rs}} = \frac{E(U)}{T_s} \quad \text{(in slot)}. \quad (28)$$

VI. Simulation Evaluation

In this section, we verify our analytical results through extensive simulations in a multi-user SRMC CRN where SUs jointly employ the GOS scheme and CH-CSMA/CA MAC for channel access. The channel access delay is evaluated in terms of channel number N, SU density per channel n and different versions of virtual carrier sensing mechanism, i.e., the conventional version VCS, the enhanced version EVCS and the optimal version OVCS. OVCS is implemented by assuming that SUs can distinguish true collision from false collision to eliminate the extra delay injected into their backoff counting-down process, from which the channel access delay performance can be regarded as the lower bound for VCS and EVCS. In order to further confirm the advantage of our designed EVCS mechanism in seizing transmission opportunity and improving channel access delay, we integrate four representative asynchronous CH rendezvous schemes (JS, ETCH-ASYN, CRSEQ and DRSEQ) with our CH-CSMA/CA MAC and present their respective performances through simulations. To the best of our knowledge, this is the first time to compare the channel access delay performance of these four asynchronous CH rendezvous schemes in the saturated transmission scenario. As the AMOCH is designed under role-based model [6], we exclude it from the comparison.

TABLE III
Protocol Parameters of PHY Layer and MAC Layer

PHY Layer	
PLCP preamble (p_{phy})	144 bits
PLCP header (h_{phy})	48 bits
Basic rate (r_{basic})	1 Mbps
Data rate (r_{data})	11 Mbps
Backoff mini-slot (σ)	20 μs
MAC Layer	
MAC header (h_{mac})	272 bits
MAC payload (l_{data})	8184 bits
SIFS	10 μs
DIFS	50 μs
RTS (l_{rts})	160 bits
CTS (l_{cts})	112 bits
ACK (l_{ack})	112 bits
CW_{min} (W_0)	32
Maximum backoff stage (m)	3
Slot (T_s)	10 ms

A. Simulation Setup

We develop a C/C++ event-driven simulator which employs the CH-CSMA/CA MAC as the MAC protocol for our considered CRNs where each SU is involved in saturated transmission state. The topology of a single-hop CRN is constructed by setting a $100m \times 100m$ topology with randomly deployed SUs of $250m$ transmission range. As existing asynchronous CH rendezvous schemes can guarantee fair access to each channel, we use SU density per channel n instead of the total number of SUs as one of the scenario parameters to indicate different intensity of multi-user contention. By using the ON-OFF channel availability model, we adjust the probability of channel availability p_a to 70% for all simulations. We repeat each simulation 20 times with identical scenario parameters and calculate the average value for each simulation result. To indicate reliability of simulation results, the confidence interval with 95% confidence level is given for each simulation result. The protocol parameters of PHY layer and MAC layer are listed in Table III by referring to 802.11b standard. Control packets (RTS, CTS and ACK) and data packets are transmitted at PHY basic rate and PHY data rate, respectively. By using the symbols parenthesized after parameters in Table III, the transmission time of data packet is $t_{data} = \frac{p_{phy}+h_{phy}}{r_{basic}} + \frac{h_{mac}+l_{data}}{r_{data}}$ and the transmission time of control packets are $t_{rts,cts,ack} = \frac{p_{phy}+h_{phy}+l_{rts,cts,ack}}{r_{basic}}$.

B. Rendezvous Statistics of the GOS Scheme

With aim at verifying our analytical results of rendezvous statistics for the GOS scheme, we construct a separate network scenario where all channels are available for simulation. As the measured metrics ETTR and EIRI are completely dominated by the hopping pattern of CHS generated in the GOS scheme, we only deploy a SU pair (one is the sender and the other is the receiver) in the network to eliminate multi-user contention. Each simulation result is denoted by the average value with 95% confidence level from 100 repeated simulations. The rendezvous statistics of the GOS scheme are shown in Fig.9, from which we can see that the analytical results of ETTR and EIRI match the corresponding simulation results very well.

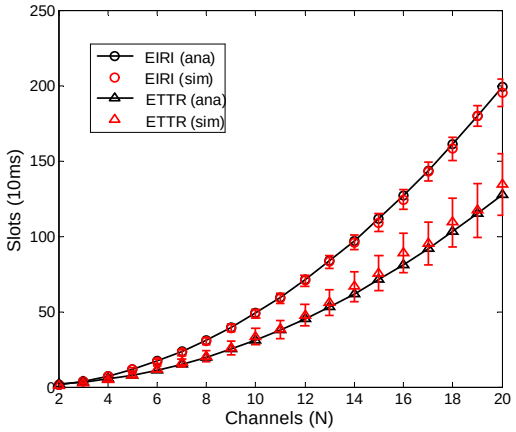

Fig. 9. Verification of rendezvous statistics for the GOS scheme

TABLE IV
VERIFICATION OF BIANCHI MODEL IN GOS BASED CH-CSMA/CA MAC

		$n=10$		$n=30$		$n=50$	
		ana	sim	ana	sim	ana	sim
$N=2$	τ	0.0174	0.009672	0.0143	0.009829	0.0127	0.009848
	p_c	0.6466	0.901728	0.7278	0.903755	0.7790	0.911141
$N=4$	τ	0.0099	0.008305	0.0095	0.008377	0.0092	0.008397
	p_c	0.8890	0.978817	0.9079	0.976686	0.9228	0.976649
$N=6$	τ	0.0087	0.00806	0.0085	0.008078	0.0084	0.008064
	p_c	0.9491	0.989526	0.9571	0.989227	0.9636	0.989661
$N=8$	τ	0.0083	0.007933	0.0082	0.007981	0.0081	0.007954
	p_c	0.9711	0.994444	0.9755	0.993429	0.9791	0.994477
$N=10$	τ	0.0081	0.007883	0.0080	0.007893	0.0080	0.007901
	p_c	0.9814	0.996317	0.9842	0.995845	0.9865	0.996313

C. The behavior of the GOS based CH-CSMA/CA MAC

The Bianchi model is well-accepted to characterize the behavior of CSMA/CA MAC in a single-channel network, but it is rare to see how to employ this model to analyze CSMA/CA MAC in a multi-channel network. As the user number on each channel of multi-channel networks may be time-varying, it seems impossible to use the Bianchi model to get the two key parameters (i.e., transmission probability τ and collision probability p_c). The reason why we can employ the Bianchi model to analyze our MAC is that we use two approximations in our analysis: (1) All SUs are distributed among channels uniformly in each slot due to the fair channel access property of CHSs designed in existing asynchronous CH rendezvous schemes; (2) Equal treatment on ETTR and EIRI, because they are of the same order of magnitude $O(N^2)$ and the difference between the coefficients of their highest order terms is small (about $1/6$). With these two approximations, we can adopt the Bianchi model to obtain the key parameters τ and p_c over each channel across slots, by regarding each channel as an independent single-channel network with n SUs.

We show the difference between analytical results derived from the modified Bianchi model and simulation results in Table IV. When channel number is not more than 4, analytical results can not match simulation results very well, especially when channel number is 2. With the increase of channel number, the analytical results match simulation results more and more precisely. One reason is that every decrement in channel number causes larger variance of SU distribution among channels and the bad case that almost all SUs jump into the same channel occurs with higher probability. By regarding the SU density per channel n as the Binomial distribution $n \sim B(M, \frac{1}{N})$, the variance $\frac{M(N-1)}{N^2}$ and the probability $(\frac{1}{N})^{M-1}$ of the worst case that all SUs jump into the same channel are both decreasing functions of channel number N. The other reason is that the disparity between $\frac{1}{ETTR+1}$ and $\frac{1}{EIRI+1}$ becomes larger with every decrement in channel number, which causes the equal treatment on $ETTR$ and $EIRI$ inappropriate in analysis.

TABLE V
IMPACT OF THE ASYNCHRONOUS CH RENDEZVOUS SCHEME ON COLLISION PROBABILITY (E.G., GOS)

	$n=2$			
	τ	p_{tc}	p_{fc}	p_c
$N=1$	0.0570	0.0570	0	0.0570
$N=2$	0.0197	0.0197	0.5747	0.5944
$N=4$	0.0101	0.0101	0.8697	0.8798
$N=6$	0.0087	0.0087	0.9367	0.9454
$N=8$	0.0083	0.0083	0.9608	0.9691

As shown in Table IV, the collision probability is extremely high. However, this consequence is caused by the employed asynchronous CH rendezvous scheme rather than the CH-CSMA/CA MAC. For a tagged SU, its false collisions only happen in slots (i.e., ETTR and EIRI) when it does not achieve rendezvous with its receiver. In order to reveal the impact of the employed asynchronous CH rendezvous scheme on collision probability, we minimize true collision of the tagged SU in slots of ETTR and EIRI by setting SU density per channel $n = 2$. In fact, we should set the total number of SUs $M = 2$ to eliminate true collision in slots of ETTR and EIRI, in which the false collision caused by asynchronous CH rendezvous schemes can be evaluated correctly. Nevertheless, it is enough to demonstrate that the high collision probability is not attributed to the CH-CSMA/CA MAC by setting $n = 2$, as true collision may happen in slots of ETTR and EIRI, which makes false collision probability lower than that when $M = 2$. The results listed in Table V are derived from (15), (16), (19) and (20) in section V-A. When channel number $N = 1$, there exists no rendezvous problem and collision probability equals to true collision probability. When $N \geq 2$, false collision dominates the collision probability, which indicates the high collision is mainly caused by the employed asynchronous CH rendezvous schemes. From this point, design of asynchronous CH rendezvous scheme for a multi-user SRMC CRN should consider how to minimize both ETTR and EIRI.

D. Probability of Seizing Transmission Opportunity

The seizing transmission opportunity performance of the GOS based CH-CSMA/CA MAC is shown in Fig.10 where the verification of our numerical analysis is also presented. When SU density per channel n increases from 10 to 50 by step 20, all the probabilities of seizing transmission opportunity under VCS, EVCS and OVCS mechanisms decrease, as the collision becomes more and more severe and it increases the failure probability of each rendezvous attempt. When the channel

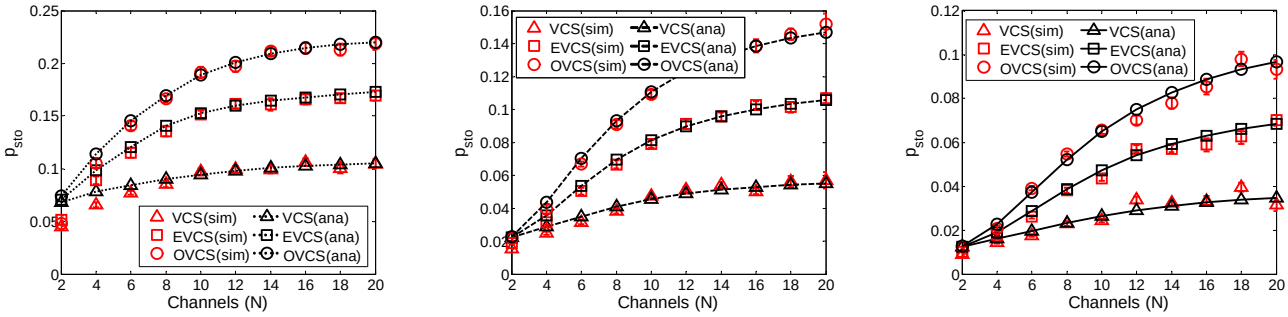

(a) n=10 (b) n=30 (c) n=50

Fig. 10. Verification of the probability of seizing transmission opportunity for the GOS scheme.

number $N \leq 8$, the probabilities of seizing transmission opportunity in analysis are higher than those in simulation, because the analytical results of collision are lower than those in simulation when N is not large enough (see Table IV). Obviously, EVCS outperforms VCS in seizing transmission opportunity. For the GOS scheme, EVCS can narrow the performance gap between VCS and OVCS by 74.84%, 53.48% and 49.08% on average when $n = 10$, 30 and 50. With the increase of channel number N, the probability of seizing transmission opportunity increases first and then levels off. The reason is that ETTR and EIRI both increase with every increment in channel number, and SUs will reach the maximum contention window size with even higher probability when they achieve rendezvous with their respective receivers. As a result, the true collision probability of SUs reduces first and remains stable when increasing channel number, which leads to the result that the probability of seizing transmission opportunity increases first and then levels off.

We integrate CRSEQ, DRSEQ, JS and ETCH_ASYN schemes with the CH-CSMA/CA MAC and present their performance of seizing transmission opportunity in Fig.11. From all results of these four schemes, EVCS can largely enhance the capability of SUs to seize transmission opportunity in comparison with VCS. It is worth noting that the probability of seizing transmission opportunity in the GOS scheme is higher than that those of the four selected schemes. Compared with the GOS scheme, these four schemes significantly improve their performance of achieving rendezvous in terms of ETTR and EIRI by shortening the period or guaranteeing more times of achieving rendezvous in a period of their designed CHSs. However, this improvement compromises the performance of seizing transmission opportunity. The reason is that when ETTR and EIRI reduces, the rendezvous probability p_{rdv} increases. When a tagged SU achieves rendezvous with its receiver, it encounters more number of its opponents (i.e., other non-tagged SUs who also achieve rendezvous with their receivers on the same channel of the tagged SU) and more intensive competition in seizing transmission opportunity.

E. Channel Access Delay

Channel access delay performance of the GOS scheme is presented and verified in Fig.12. We also present this performance in three cases by setting $n = 10$, 30 and 50.

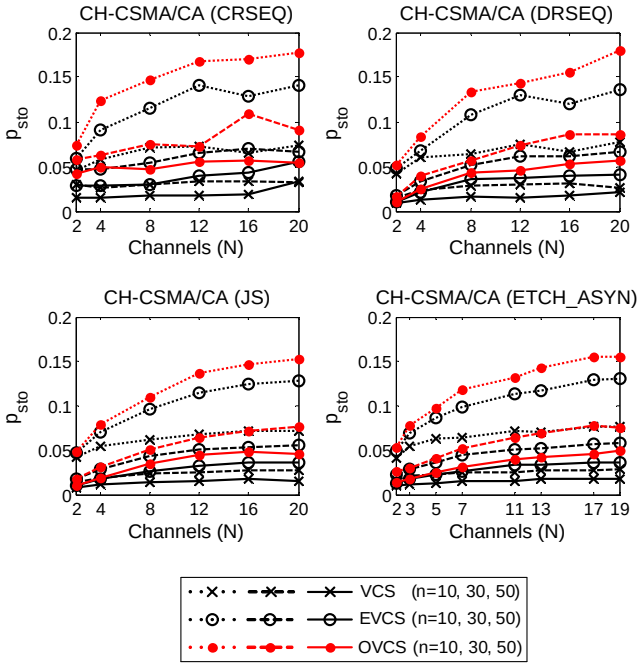

Fig. 11. Impact of different virtual carrier sensing mechanisms on probability of seizing transmission opportunity for the four selected schemes

The channel access delay increases as expected with n as collision becomes more and more severe. By comparison, EVCS narrows the performance gap between VCS and OVCS by 74.73%, 69.10%, and 68.21% on average when $n = 10$, 30 and 50. Therefore, EVCS can effectively alleviate the impact of false collision problem on channel access delay.

For the four selected schemes, their channel access delay performances are all improved significantly under EVCS (see Fig.13). Unlike VCS, EVCS can effectively suppress the increase trend of channel access delay with every increment in channel number for these four schemes. Especially, EVCS can reduce channel access delay about an order of magnitude when n=50. Note that channel access delay under EVCS approximates to that under OVCS when n=10 and the performance gap between them is still small even when n=50, which proves the effectiveness of EVCS on improving channel access delay.

It is noteworthy that these four schemes are inferior to the

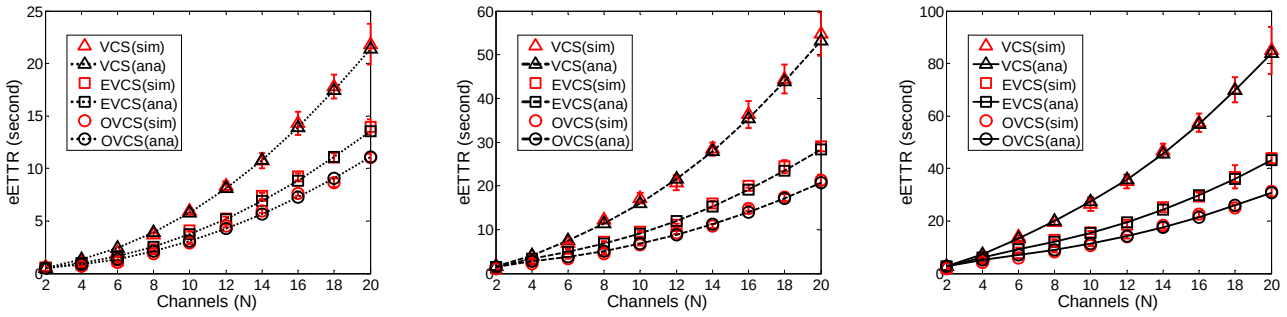

(a) n=10 (b) n=30 (c) n=50

Fig. 12. Verification of the channel access delay for the GOS scheme.

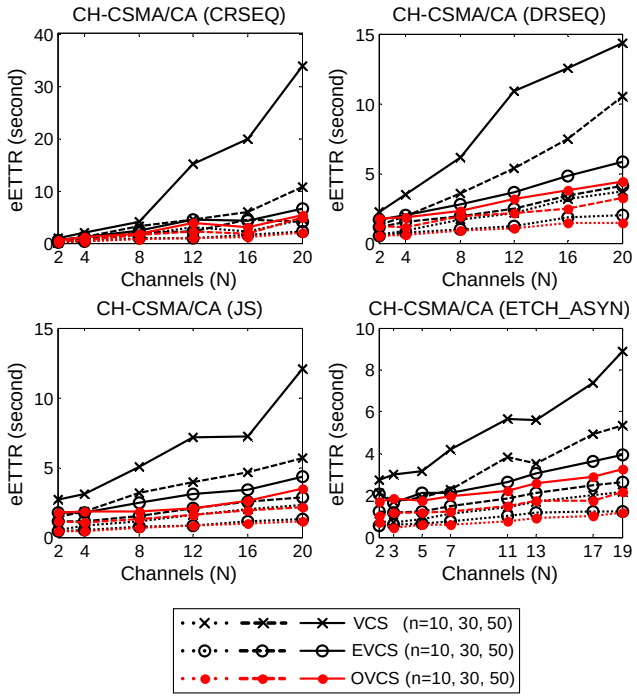

Fig. 13. Impact of different virtual carrier sensing mechanisms on channel access delay for the four selected schemes

GOS scheme in terms of seizing transmission opportunity, but they outperform the GOS scheme significantly in terms of channel access delay. The reason is that given the channel availability probability and SU density per channel, the channel access delay is an increasing function of ETTR and EIRI. Therefore, it is advisable for recent asynchronous CH rendezvous schemes to take ETTR as the main performance metric, as it is conducive to improving channel access delay. Even so, it is should be noted that ETTR is in milliseconds (e.g., with hop slot duration $T_s = 10ms$, the ETTRs of DRSEQ, JS and ETCH are $O(N)$ hop slots and in milliseconds under symmetric model), but it cannot ensure that eETTR is also in milliseconds when taking into account the effect of channel availability and multi-user contention. From the simulation results, eETTR is in seconds and it is not satisfactory as the networking performance.

VII. Conclusions

In this paper, channel access delay was investigated in saturated transmission scenario for single-hop multi-user SRMC CRNs based on asynchronous CH rendezvous schemes and CSMA/CA MAC. A random access based MAC named CH-CSMA/CA MAC was tailored from IEEE 802.11 DCF to work with existing asynchronous CH rendezvous schemes, in which the proposed EVCS mechanism can effectively alleviate the negative impact of the false collision problem on channel access delay. Moreover, a modified Bianchi model and an AMC model were employed jointly to analyze the channel access delay performance by considering the aggregate effect of the used asynchronous CH rendezvous scheme, dynamic channel availability and the MAC protocol, which was verified through extensive simulations. In this paper, we found that the metric EIRI ignored in existing research work also significantly impacts the channel access delay and the mainly concerned metric ETTR is insufficient to guarantee satisfactory channel access delay.

From this work, there are two insights into the improvement of the channel access delay. One is to mitigate the impact of the logical partition problem on channel access delay, but this problem has not been well studied so far. The other is to further reduce the rendezvous delay of CH based rendezvous schemes. We have proposed a neighbor cooperation framework [33] to improve the rendezvous delay of existing asynchronous CH rendezvous schemes. As our future work, we will study how to employ this framework to improve the performance of channel access delay. To obtain insightful quality of service (QoS) of existing asynchronous CH rendezvous schemes, queuing theory is an recommendable tool to study the relationship between the traffic arrival rate and the packet queuing delay. As existing queuing theory based research work [34] [35] paid little attention to the effect of the rendezvous problem, it is also an interesting problem to study the queuing delay by integrating existing CH based rendezvous schemes.

Appendix
Derivation of Invalid Rendezvous Patterns $\{x^*\}$

As it is analytically intractable to formulate the relationship between channel number N and invalid rendezvous patterns $\{x^*\}$, we refer to the method of finding rendezvous regularities which is used in the GOS scheme (see appendix in [10]). We

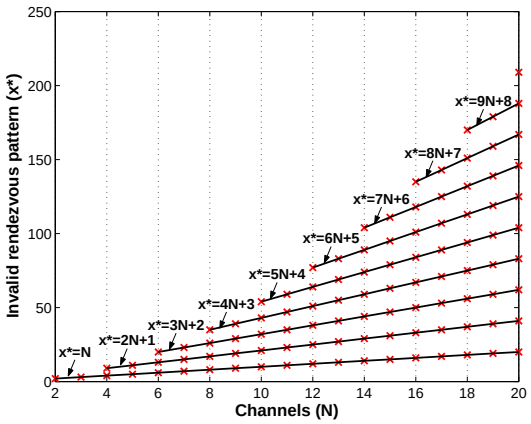

Fig. 14. Invalid rendezvous patterns in GOS scheme

simulate the GOS scheme in different two-user scenarios by changing channel number $N \in [2, 20]$. In each scenario, we record the rendezvous patterns through altering the effective clock offset $\Delta \in \{0, 1, \cdots, N(N+1)-1\}$ between the rendezvous pair and acquire the invalid rendezvous patterns.

From Fig.14, we get two laws to extend $\{x^*\}$ derivation for general case: (1) The number of invalid rendezvous patterns $\kappa = |\{x^*\}| = \lfloor \frac{N}{2} \rfloor$; (2) By arranging all invalid rendezvous patterns in $\{x^*\}$ in ascending order, $\min(\{x^*\})$ is N and the difference between any two adjacent invalid rendezvous patterns is $N+1$, which is illustrated by the linear functions showed in Fig.14. Then, for each channel number N, we get the general term formula of $\{x^*\}$

$$\{x^* | N + (\kappa - 1)(N+1), \kappa \in \{1, 2, \cdots, \left\lfloor \frac{N}{2} \right\rfloor\}\}$$

There are two critical values for effective clock offset Δ. One is zero, the other is $\frac{N(N+1)}{2}$. When $\Delta = 0$, the CHSs of a rendezvous pair completely coincide, but this rendezvous pattern does not appear when $\Delta \neq 0$. Due to the periodicity of CHSs, the rendezvous pattern under $\Delta = \frac{N(N+1)}{2} - \delta$ is equivalent to that under $\Delta = \frac{N(N+1)}{2} + \delta$, where $\delta \in \{1, 2, \cdots, \frac{N(N+1)}{2} - 1\}$. When $\Delta = \frac{N(N+1)}{2}$, the special rendezvous pattern $[x, y]$ satisfies $x = y = \frac{N(N+1)}{2} - 1$ and it appears only once when N is odd (see Fig.5 and result in (8)). When N is even, $\kappa = \lfloor \frac{N}{2} \rfloor = \frac{N}{2}$, then

$$\begin{aligned} x^* &= N + (\kappa - 1)(N+1) \\ &= \kappa(N+1) - 1 \\ &= \frac{N(N+1)}{2} - 1 \end{aligned}$$

which indicates the special rendezvous pattern $[x, y{=}x]$ becomes invalid in case that N is even (see in (9)).

ACKNOWLEDGMENT

The authors would like to thank the anonymous reviewers for their very insightful comments. The work in this paper was supported by the National Natural Science Foundation of China (NSFC) under grant No.61070203 and 61172066, the Ministry of Education (MOE) Program for New Century Excellent Talents, and Oriental Scholar Program of Shanghai Municipal Education Commission.

REFERENCES

[1] I. Akyildiz, W. Lee, M. Vuran, and S. Mohanty, "Next generation/dynamic spectrum access/cognitive radio wireless networks: a survey," *Computer Networks*, vol. 50, no. 13, pp. 2127–2159, 2006.

[2] S. Haykin, "Fundamental issues in cognitive radio," in *Cognitive Wireless Communication Networks*, E. Hossain and V. Bhargava, Eds. Springer US, 2007, pp. 1–43.

[3] J. Mo, H. So, and J. Walrand, "Comparison of multi-channel mac protocols," in *Proceedings of the 8th ACM international symposium on Modeling, analysis and simulation of wireless and mobile systems*. ACM, 2005, pp. 209–218.

[4] A. De Domenico, E. Strinati, and M.-G. Di Benedetto, "A survey on mac strategies for cognitive radio networks," *Communications Surveys Tutorials, IEEE*, vol. 14, no. 1, pp. 21–44, Quarter 2012.

[5] Y.-C. Liang, K.-C. Chen, G. Li, and P. Mahonen, "Cognitive radio networking and communications: An overview," *Vehicular Technology, IEEE Transactions on*, vol. 60, no. 7, pp. 3386–3407, Sept. 2011.

[6] N. Theis, R. Thomas, and L. DaSilva, "Rendezvous for cognitive radios," *Mobile Computing, IEEE Transactions on*, vol. 10, no. 2, pp. 216–227, 2011.

[7] H. Liu, Z. Lin, X. Chu, and Y.-W. Leung, "Taxonomy and challenges of rendezvous algorithms in cognitive radio networks," in *Computing, Networking and Communications (ICNC), 2012 International Conference on*, 2012, pp. 645–649.

[8] K. Bian, J. Park, and R. Chen, "A quorum-based framework for establishing control channels in dynamic spectrum access networks," in *MobiCom*, 2009, pp. 25–36.

[9] Y. Zhang, Q. Li, G. Yu, and B. Wang, "Etch: Efficient channel hopping for communication rendezvous in dynamic spectrum access networks," in *INFOCOM, 2011 Proceedings IEEE*, 2011, pp. 2471–2479.

[10] L. DaSilva and I. Guerreiro, "Sequence-based rendezvous for dynamic spectrum access," in *New Frontiers in Dynamic Spectrum Access Networks, 2008. DySPAN 2008. 3rd IEEE Symposium on*, 2008, pp. 1–7.

[11] K. Bian and J. Park, "Maximizing rendezvous diversity in rendezvous protocols for decentralized cognitive radio networks," *Mobile Computing, IEEE Transactions on*, vol. PP, no. 99, p. 1, 2012.

[12] H. Liu, Z. Lin, X. Chu, and Y. Leung, "Jump-stay rendezvous algorithm for cognitive radio networks," *Parallel and Distributed Systems, IEEE Transactions on*, vol. PP, no. 99, p. 1, 2012.

[13] J. Shin, D. Yang, and C. Kim, "A channel rendezvous scheme for cognitive radio networks," *Communications Letters, IEEE*, vol. 14, pp. 954–956, 2010.

[14] D. Yang, J. Shin, and C. Kim, "Deterministic rendezvous scheme in multichannel access networks," *Electronics Letters*, vol. 46, no. 20, pp. 1402–1404, September 2010.

[15] H. Su and X. Zhang, "Channel-hopping based single transceiver mac for cognitive radio networks," in *Information Sciences and Systems, 2008. CISS 2008. 42nd Annual Conference on*, March 2008, pp. 197–202.

[16] P. Pawelczak, S. Pollin, H.-S. So, A. Bahai, R. Prasad, and R. Hekmat, "Performance analysis of multichannel medium access control algorithms for opportunistic spectrum access," *Vehicular Technology, IEEE Transactions on*, vol. 58, no. 6, pp. 3014–3031, July 2009.

[17] J. Park, P. Pawelczak, and D. Cabric, "Performance of joint spectrum sensing and mac algorithms for multichannel opportunistic spectrum access ad hoc networks," *Mobile Computing, IEEE Transactions on*, vol. 10, no. 7, pp. 1011–1027, July 2011.

[18] A. T. Hoang, D. Wong, and Y.-C. Liang, "Design and analysis for an 802.11-based cognitive radio network," in *Wireless Communications and Networking Conference, 2009. WCNC 2009. IEEE*, April 2009, pp. 1–6.

[19] Y. H. Bae, A. Alfa, and B. D. Choi, "Performance analysis of modified ieee 802.11-based cognitive radio networks," *Communications Letters, IEEE*, vol. 14, no. 10, pp. 975–977, October 2010.

[20] S. Kumar, N. Shende, C. Murthy, and A. Ayyagari, "Throughput analysis of primary and secondary networks in a shared ieee 802.11 system," *Wireless Communications, IEEE Transactions on*, vol. PP, no. 99, pp. 1–12, 2013.

[21] J. W. Chong, Y. Sung, and D. K. Sung, "Rawpeach: Multiband csma/ca-based cognitive radio networks," *Communications and Networks, Journal of*, vol. 11, no. 2, pp. 175–186, April 2009.

[22] R. Hasan and M. Murshed, "Unsaturated throughput analysis of a novel interference-constrained multi-channel random access protocol for cognitive radio networks," in *Personal Indoor and Mobile Radio Communications (PIMRC), 2012 IEEE 23rd International Symposium on*, Sept. 2012, pp. 178–184.
[23] K. J. Kim, K. S. Kwak, and B. D. Choi, "Performance analysis of opportunistic spectrum access protocol for multi-channel cognitive radio networks," *Communications and Networks, Journal of*, vol. 15, no. 1, pp. 77–86, 2013.
[24] G. Bianchi, "Performance analysis of the ieee 802.11 distributed coordination function," *Selected Areas in Communications, IEEE Journal on*, vol. 18, no. 3, pp. 535–547, March 2000.
[25] C. M. Grinstead and J. L. Snell, *Introduction to probability*. American Mathematical Soc., 1998.
[26] C.-M. Lee, J.-S. Lin, K.-T. Feng, and C.-J. Chang, "Design and analysis of transmission strategies in channel-hopping cognitive radio networks," *Mobile Computing, IEEE Transactions on*, vol. 11, no. 10, pp. 1569–1584, Oct 2012.
[27] P. Bahl, R. Chandra, and J. Dunagan, "Ssch: slotted seeded channel hopping for capacity improvement in ieee 802.11 ad-hoc wireless networks," in *Proceedings of the 10th annual international conference on Mobile computing and networking*, ser. MobiCom'04. New York, NY, USA: ACM, 2004, pp. 216–230.
[28] Q. Zhao, L. Tong, A. Swami, and Y. Chen, "Decentralized cognitive mac for opportunistic spectrum access in ad hoc networks: A pomdp framework," *Selected Areas in Communications, IEEE Journal on*, vol. 25, no. 3, pp. 589–600, April 2007.
[29] K. Tan, H. Liu, J. Zhang, Y. Zhang, J. Fang, and G. M. Voelker, "Sora: high-performance software radio using general-purpose multi-core processors," *Commun. ACM*, vol. 54, pp. 99–107, jan 2011.
[30] C. de M. Cordeiro, K. S. Challapali, D. Birru, and S. S. N., "Ieee 802.22: An introduction to the first wireless standard based on cognitive radios," *Journal of Communications*, vol. 1, no. 1, pp. 38–47, 2006.
[31] H. Su and X. Zhang, "Cross-layer based opportunistic mac protocols for qos provisionings over cognitive radio wireless networks," *Selected Areas in Communications, IEEE Journal on*, vol. 26, no. 1, pp. 118–129, 2008.
[32] M. Gast, *802.11 wireless networks: The definitive guide*. Southeast University Press, 2006.
[33] Q. Liu, D. Pang, G. Hu, X. Wang, and X. Zhou, "A neighbor cooperation framework for time-efficient asynchronous channel hopping rendezvous in cognitive radio networks," in *Dynamic Spectrum Access Networks (DYSPAN), 2012 IEEE International Symposium on*, 2012, pp. 529–539.
[34] S. Wang, J. Zhang, and L. Tong, "Delay analysis for cognitive radio networks with random access: A fluid queue view," in *INFOCOM, 2010 Proceedings IEEE*, 2010, pp. 1–9.
[35] A. Laourine, S. Chen, and L. Tong, "Queuing analysis in multichannel cognitive spectrum access: A large deviation approach," in *INFOCOM, 2010 Proceedings IEEE*, 2010, pp. 1–9.

Quan Liu received his B. Eng. degree in 2007 from Central South University (CSU) and finished his master program in 2009 at National University of Defense Technology (NUDT), both in China. He is currently working toward a Ph.D. degree with the College of Computer Science at NUDT and jointly trained at Wang Lab of University of Michigan-Shanghai Jiao Tong University (UM-SJTU) Joint Institute, Shanghai Jiao Tong University. His research interests are in distributed coordination, MAC protocol design and cognitive networking in cognitive radio networks. He is a student member of ACM and China Computer Federation (CCF).

Xudong Wang (SM'8) received the Ph.D. degree in electrical and computer engineering from Georgia Institute of Technology, Atlanta, GA, USA, in 2003.

He has been with several companies as a Senior Research Engineer, a Senior Network Architect, and an R&D Manager. He is currently with the University of Michigan-Shanghai Jiao Tong University (UM-SJTU) Joint Institute, Shanghai Jiao Tong University, Shanghai, China. He is a Distinguished Professor (Shanghai Oriental Scholar) and is the Director of the Wireless And Networking (WANG) Laboratory. He is also an affiliate faculty member with the Department of Electrical Engineering, University of Washington, Seattle, WA, USA. He has been actively involved in R&D, technology transfer, and commercialization of various wireless networking technologies. He holds a number of patents on wireless networking technologies, and most of his inventions have been successfully transferred to products. His research interests include wireless communication networks, smart grid, and cyber physical systems.

Dr. Wang was a voting member of the IEEE 802.11 and 802.15 Standards Groups. He is an Editor of the IEEE TRANSACTIONS ON VEHICULAR TECHNOLOGY, Elsevier *Ad Hoc Networks*, and ACM/Kluwer *Wireless Networks*. He has been a Guest Editor of several journals. He was the demo Co-Chair of the ACM International Symposium on Mobile Ad Hoc Networking and Computing (ACM MOBIHOC 2006), a Technical Program Co-chair of the Wireless Internet Conference (WICON) 2007, and a General Co-chair of WICON 2008. He has been a Technical Committee Member of many international conferences.

Biao Han received his B. Eng. degree and finished his master program in 2007 and 2009 respectively, both at National University of Defense Technology (NUDT). He is currently working toward a Ph.D. degree with the Graduate School of Systems and Information Engineering at University of Tsukuba, Japan. His research interests are in cross-layer optimization, green networking, cooperative communication in wireless networks. He is a student member of IEEE and China Computer Federation (CCF).

Xiaodong Wang received the BE, ME, and Ph.D. degrees in computer science in 1994, 1998, and 2001, respectively, all from the National University of Defence Technology (NUDT), Changsha, China. His main research interests are wireless networks and mobile computing, including mobile ad hoc networks and wireless sensor networks. He is a member of the IEEE Communication Society, IEEE, and China Computer Federation (CCF).

Xingming Zhou has been with National University of Defence Technology (NUDT) since 1978, where he is currently the head of scholar committee of National Key Laboratory on Parallel and Distributed Processing. He has been the academician of Chinese Academy of Science (CAS) since 1992. He has been the co-chair of many international conferences and workshops on parallel computing, network computing, and mobile networks. His current research interests include high-performance computing and network computing. He is a senior member of China Computer Federation (CCF).